Hufnagel, A, Fernandez-Twinn, DS, Blackmore, HL, Ashmore, TJ, Heaton, RA, Jenkins, B, Koulman, A, Hargreaves, IP, Aiken, CE and Ozanne, SE

Maternal but not fetoplacental health can be improved by metformin in a murine diet-induced model of maternal obesity and glucose intolerance

Maternal but not fetoplacental health can be improved by metformin in a murine diet-induced model of maternal obesity and glucose intolerance

Antonia Hufnagel[1,4,6,*], **Denise S Fernandez-Twinn**[1,4], Heather L Blackmore[1], Thomas J Ashmore[1], Robert A Heaton[2], Benjamin Jenkins[1], Albert Koulman[1], Iain P Hargreaves[2], Catherine E Aiken[3], Susan E Ozanne[1,5]

1. University of Cambridge Metabolic Research Laboratories and MRC Metabolic Diseases Unit, Wellcome Trust-MRC Institute of Metabolic Science, Level 4, Addenbrooke's Hospital, Cambridge, Cambridgeshire, United Kingdom, CB22 0QQ.
2. School of Pharmacy and Biomolecular Sciences, Liverpool John Moores University, Liverpool L3 3AF, UK.
3. Department of Obstetrics and Gynaecology, University of Cambridge, Cambridge, United Kingdom; National Institute for Health Research Cambridge Biomedical Research Centre, Cambridge, University of Cambridge, United Kingdom.
4. These authors contributed equally to this work
5. Senior author
6. Lead contact

*corresponding author: Antonia Hufnagel, ash56@medschl.cam.ac.uk

Table of contents category: Placenta, Pregnancy and Perinatal Physiology

Running title: A murine model of obesity, diabetes and metformin during pregnancy

Key words: developmental programming, gestational diabetes mellitus, maternal obesity, metformin, placenta

Key Points summary (147 words)

- Maternal obesity and gestational diabetes mellitus have detrimental short- and long-term effects for mother and child.
- Metformin is commonly used to treat gestational diabetes mellitus in many populations worldwide but the effects on fetus and placenta are unknown.
- In a mouse model of diet-induced obesity and glucose intolerance in pregnancy we show reduced uterine artery compliance, placental structural changes and reduced fetal growth.
- Metformin treatment improved maternal metabolic health and uterine artery compliance but did not rescue the obesity-induced changes in the fetus or the placenta. Metformin crossed the placenta into the fetal circulation and entered fetal tissue in high quantities.
- Metformin has beneficial effects on maternal health beyond glycaemic control. But despite improvements in maternal physiology, metformin did not prevent fetal growth restriction or placental ageing. The high uptake of metformin into the placental and fetal circulation highlights the potential for direct effects of metformin on the fetus and the offspring later in life.

Abstract (249 words)

Maternal obesity is a global problem that increases the risk of short- and long-term adverse outcomes for mother and child, many of which are linked to gestational diabetes mellitus. Effective treatments are essential to prevent the transmission of poor metabolic health from mother to child. Metformin is an effective glucose lowering drug commonly used to treat gestational diabetes mellitus; however, its wider effects on maternal and fetal health are poorly explored. In this study we used a mouse (C57Bl6/J) model of diet-induced (high sugar/high fat) maternal obesity to explore the impact of metformin on maternal and feto-placental health. Metformin (300 mg/kg/day) was given to obese females via the diet one week prior to mating and throughout pregnancy which was shown to achieve a clinically-relevant concentration in the maternal serum (1669 ± 568 nM at the end of pregnancy). Obese dams developed glucose intolerance during pregnancy and had reduced uterine artery compliance (p=0.003 vs control dams). Metformin treatment of obese dams improved maternal glucose tolerance, reduced maternal fat mass, and restored uterine artery function. Placental efficiency was reduced in obese dams, with increased calcification and reduced labyrinthine area. Consequently, fetuses from obese dams weighed less at the end of gestation (E18.5, 0.93±0.07g in obese vs. 1.16±0.03g in control fetuses, n=14 litters for both groups, p<0.001). Despite normalisation of maternal parameters, metformin did not correct placental structure or fetal growth restriction (fetal weight at E18.5: 0.96±0.11g, n=13 litters). Metformin levels were substantial in the placenta and fetal circulation (109.7±125.4 nmol/g in the placenta and 2.06±2.33 nmol/mL in fetal plasma). These findings reveal the distinct effects of metformin administration during pregnancy on mother and fetus and highlight the complex balance of risk versus benefits that are weighed in obstetric medical treatments.

Introduction

The growing prevalence of obesity worldwide means that in many populations at least 50% of women are overweight or obese at the start of pregnancy (Hill *et al.*, 2019). Obesity during pregnancy is associated with increased risk of complications, including preeclampsia, preterm delivery, stillbirth, and importantly gestational diabetes mellitus (GDM) (Stephenson *et al.*, 2018). It is now estimated that the prevalence of GDM ranges from 1% to 30% worldwide (David McIntyre *et al.*, 2019).

Maternal obesity and untreated GDM during pregnancy have direct effects on the fetus, with implications for long-term offspring health (Alfaradhi & Ozanne, 2011). Observational studies in humans show increased risks of obesity (Hu *et al.*, 2019), type 2 diabetes (Lahti-Pulkkinen *et al.*, 2019), and cardiovascular disease (Gaillard, 2015) in offspring born to obese mothers and those with GDM (Mitanchez *et al.*, 2015). Studies in animal models by our laboratory and others have shown previously that these relationships are causal. These studies demonstrate that obesity and/or glucose intolerance during pregnancy lead to cardiac dysfunction (Blackmore *et al.*, 2014), insulin resistance (Isganaitis *et al.*, 2014), hyperphagia (Steculorum & Bouret, 2011), obesity (Samuelsson *et al.*, 2008) and fatty liver (Alfaradhi *et al.*, 2014) in young adult offspring. However, the mechanisms linking fetal development and growth in affected pregnancies with long-term adverse effects are complex and yet to be fully understood.

The placenta is the key interface between the mother and fetus, and therefore a likely mediator of the effects of maternal health on the developing fetus. Studies in humans and in animal models have shown that placentas from obese pregnancies display lipotoxicity (Jarvie *et al.*, 2010), inflammation (Pantham *et al.*, 2015), and have reduced placental vessel density (Hayes *et al.*, 2012), highlighting that the protective capacities of the placenta can be exhausted in diabetic and/or obese pregnancies (Desoye & Wells, 2021).

Interventions need to be carefully assessed to improve maternal and fetal health. Lifestyle and dietary interventions are generally the first recommendation to treat GDM, and are successful in >50% of women (ADA, 2019). If these interventions fail, pharmacological interventions such as metformin, glyburide, or insulin are implemented (SMFM, 2018). Metformin, a biguanide with glucose-lowering actions, is a pragmatic alternative to insulin as it can be taken orally, does not need to be refrigerated, and does not cause hypoglycaemic episodes (Gray *et al.*, 2017). In the UK, National Institute for

Health and Care Excellence (NICE) guidelines recommend metformin as a first-line drug therapy for GDM (NICE, 2015) whereas other countries, such as Germany and Turkey (Schäfer-Graf *et al.*, 2018; SEMT, 2019), are much more cautious regarding metformin use in pregnancy.

It is well-established that metformin treatment of GDM improves glycaemic control in the mother and is associated with reduced gestational weight gain (Syngelaki *et al.*, 2016). However, there is relatively little data regarding immediate or long-term effects of maternal metformin use on the offspring (Tarry-Adkins *et al.*, 2019). Unlike insulin, metformin freely crosses the placenta and reaches circulating concentrations in the fetus that match those in the mother (Priya & Kalra, 2018). Human studies looking at polycystic ovary syndrome, GDM, and type 2 diabetes pregnancies suggest that intrauterine metformin exposure leads to reduced birthweight followed by increased adiposity later in childhood (Rowan *et al.*, 2011; Guro *et al.*, 2018; Feig *et al.*, 2020). However data on immediate effects of metformin on the fetus and placental function are scarce (Tarry-Adkins *et al.*, 2019). But metformin could have potential negative effects on the placenta and fetal development due to its inhibition of the mTOR pathway, cell proliferation and mitochondrial function (Lindsay & Loeken, 2017).

We addressed this knowledge gap by characterising maternal metabolic health, fetal growth, and placental structure and function using a murine model of metformin treatment for diet-induced obesity and glucose intolerance in pregnancy.

Methods

Ethical approval

Animal studies were approved by the animal welfare ethical review process of the University of Cambridge (UK Animals Scientific Procedures Act 1986). The study was performed under the animal project licence P5FDF0206 issued by the UK Home Office and complies with the standards stated for the Journal of Physiology (Grundy, 2015).

Animal work

A model of maternal diet-induced obesity that is well-established in our laboratory and is described in detail elsewhere (Fernandez-Twinn *et al.*, 2012) was used. Mice were purchased from Charles River Laboratories (Cat#000664, RRID: IMSR_JAX:000664) and bred in house. After weaning at 3 weeks of age, female C57Bl6/J mice were fed *ad libitum* either an obesogenic diet high in sugar and fat (10% simple sugars, 20% animal fat, 23% protein [w/w], 4.5 kcal/g, Special Dietary Services, Cat #824053) together with condensed milk in glass pots (55% simple sugar, 8% fat, 8% protein [w/w], 3.2 kcal/g, Nestle, Cat #12029969) and a mineral mix (MP Biomedicals, Cat #AIN93G) or a control chow diet (RM1, 7% simple sugars, 3% fat, 15% protein [w/w], 3.5 kcal/g, Special Dietary Services, Cat #801002). In this model there is no difference in protein intake between the groups as shown previously (Samuelsson *et al.*, 2008; Maragkoudaki *et al.*, 2020). Assignment of dietary groups was carried out by an animal technician who was not involved in any of the subsequent physiological or molecular analyses. Mice were then mated for a first pregnancy at 6 weeks of age after which they were allowed at least one week of rest for recovery. Animals on a control diet were mated for the second experimental pregnancy with a body weight ≤25 g. Mice fed an obesogenic diet were mated or dosed with metformin once they reached a body weight of ≥35 g. For all groups this was at approximately at 18 weeks of age. Based on power calculations 13-14 mice were used per group. Mice were single-housed and kept in individually ventilated cages with wood chip bedding, free access to food, water, and environmental enrichment (nesting material and a tunnel) in a 12 h light/dark cycle. Metformin (MP Biomedicals Cat #02151691-CF) was administered one week prior to mating and throughout pregnancy in the condensed milk. Weighing of condensed milk twice a week allowed the calculation and adjustment of metformin intake in mg/kg/day. The average dose that animals received was 255.2 ± 48.0 mg/kg/day, which lies in the desired range of 200 - 300 mg/kg/day, based on clinically relevant doses (Salomäki *et*

al., 2013). Liquid chromatography - mass spectrometry (LC-MS) showed the mean serum metformin concentration was 1669 ± 568 nM, which falls within the clinical range reported in human pregnancies (Liao *et al.*, 2020). The study was designed to address whether intervention with metformin can improve detrimental effects of a pregnancy complicated by obesity and GDM, therefore no metformin-treated control group was used. As metformin is not given to lean pregnant women this is not clinically relevant. This is in line with the ARRIVE guideline (NC3Rs) so that the minimal number of animals needed is used.

Intraperitoneal GTT

Dams were fasted for 4 hours on the morning of embryonic day E17.5. Glucose (1mg/kg) was injected intraperitoneally, and blood glucose levels measured at 0, 15, 30, 60 and 120 minutes using a glucometer (AlphaTRAK, Abbot Logistics). Due to the high variability in the ipGTT power calculations showed that higher n numbers are needed for this outcome measure compared to all others, therefore 16 control, 20 obese and 19 metformin dams were included in this analysis. Collection of tail blood was performed at 0 minutes into capillary tubes (Hirschmann-Laborgeräte). Glucose curves are shown as percentage of starting glucose. If the glucose levels rose less than 50% between fasting and timepoint 15 and or 30 minutes the GTT data was excluded. Insulin was measured with the Crystal Chem Mouse Insulin ELISA (Ultra-Sensitive) kit (Cat #90080). The HOMA-IR was calculated according to the following formula: fasting insulin [mU/l] x fasting glucose [mmol/l]/22.5.

Fat mass assessment

Fat mass at E18.5 was assessed via Time Domain Nuclear Magnetic Resonance (TD-NMR, Bruker) measurements.

Ultrasound assessments

Uterine, umbilical and fetal middle cerebral artery function were assessed via ultrasound in the morning of day E18.5 (FUJIFILM VisualSonics, Vevo3100). Anaesthesia in the dams was induced with 2% isoflurane and then maintained at 1.5% isoflurane. Isoflurane is commonly used in ultrasound as it affects heart and respiration rate the least compared to other anaesthetics (Janssen *et al.*, 2004). Mice were placed on a heated platform, the electrocardiogram monitored and body temperature measured via a rectal probe and kept at around 36°C throughout. Uterine artery Doppler measurements were obtained by using the bladder and the split of the uterine and iliac artery from the

abdominal aorta as landmarks (Zhang & Croy, 2009). The pulsatility and resistance index of the uterine artery were corrected for maternal heart rate (Ochi *et al.*, 2003). Both indices are a surrogate measure for the vessel resistance and vascular compliance (Holmgren *et al.*, 2020). The umbilical artery was measured in a free loop transverse section (Hernandez-Andrade *et al.*, 2014). Scanned fetuses were marked on the skin of the dam so that they could be identified and sexed upon dissection. The Placental Pulsatility Index (PPI) was calculated using the following formula: PPI = (uterine artery PI + umbilical artery PI)/2 (Gudmundsson *et al.*, 2017). Analysis of the ultrasound recordings was performed with the VevoLab software.

Dissections

After the ultrasound measurements were taken, cardiac puncture was performed under 2% isoflurane anaesthesia and death confirmed by cervical dislocation. Tissues of the dams were collected, and fetuses and placentas dissected out. Fetal weight was recorded, and biometry measured with a caliper. Amniotic fluid was taken from the intact amniotic sac via a syringe. Fetal blood was obtained by collecting the blood after decapitation into capillary tubes. Fetal liver and kidneys were dissected out. Fetuses were sexed visually by detection of a black spot between tail and genital tubercle present in male fetuses (Deeney *et al.*, 2016) and subsequently confirmed via molecular analysis based on a protocol from McFarlane et al. (Mcfarlane *et al.*, 2013). Briefly, genomic DNA was isolated, and PCR performed (GO Taq G2 DNA polymerase from Promega, Cat #PAM7841, annealing temperature 57°C) with the following primer: SX_F, 5′-GATGATTTGAGTGGAAATGTGAGGTA-3′; SX_R, 5′-CTTATGTTTATAGGCATG CACCATGTA-3′. On an agarose gel male samples display one band at 280bp, female samples show 2-3 bands (480bp, 660bp, 685bp).

sFlt measurement

sFlt (VEGF-R1) was measured in maternal serum by ELISA according to the manusfacturer's instructions (R and D Systems, Cat #MVR100).

Histology (liver and placenta)

Dam livers and placentas were immersion-fixed in 10% formalin and processed. Dam liver sections (one mid-section, 5µm) were stained with Haematoxylin and Eosin and fat vacuole content quantified with the HALO software (Indica labs). Artificial intelligence of the software was used to exclude vessels for the subsequent analysis of the fat vacuoles, via the HALO vacuole quantification module.

Placental sections (one mid-section, 5 µm) were deparaffinised and rehydrated and incubated in water for 15 mins. at 60°C. Antigen retrieval was performed (97°C, pH=9, 20 mins., Vector, Cat #H-3301) and the slides blocked with 1x animal-free blocking solution for 1 hour (Vector, Cat #SP-5030). Slides were incubated with the primary antibodies for CD31 and Tpbpa (R+D, Cat #AF3628, RRID: AB_2161028 1:40 dilution and abcam, Cat #ab104401, RRID: AB_10901888, 1:1000 dilution in antibody diluent (Vector, Cat #SP-5035)) overnight at 4°C. After washing (0.5% Tween in TBS, T-TBS) the secondary antibodies were applied subsequently for 1 hour at room temperature (first NL557 (R+D, Cat# NL001, RRID: AB_663766) at 1:200, then Alexa488 (Invitrogen, Cat# A11008, RRID: AB_143165) at 1:1000). After washes in T-TBS and PBS slides were stained with DAPI for 10 min. in the dark and TrueVIEW quenching solution (Vector, SP-4800) was subsequently used according to the protocol. Slides were mounted in Vectashield hard set anti-fade mounting medium (Vector, Cat #H-1400). Analysis of the slides was performed blinded with HALO software by manually delineating the placental layers.

To analyse placental calcification, Alizarin Red staining was performed (Orchard, 2013). Sections were dewaxed and immediately put into 95% alcohol, slides were air-dried and incubated in Alizarin Red (Sigma-Aldrich, Cat #A-5533) solution for 5 minutes (1% aqueous solution pH=6.4, ammonium hydroxide). After rinsing under water, slides were counterstained with fast green (0.05% FCF (Sigma-Aldrich, Cat #F-7252) in 0.2% acetic acid for 15 seconds). Slides were washed under water, dehydrated, cleared and mounted in synthetic resin. Slides were analysed automatically via the HALO software with a classifier programmed to count Alizarin Red positive and negative areas within the manually delineated whole placental section.

Quantitative RT-PCR

RNA from placentas, fetal livers and kidneys (5 mg) was extracted with a miRNeasy Micro kit (Qiagen, Cat #217084), 1 fetus per sex and litter with an n of 3 was used. Fetal liver and kidney were chosen as two metabolic tissues that can be clearly dissected out in the E18.5 fetus. DNA was digested on column with a DNase Qiagen set (Qiagen, Cat #79254). After reverse transcription (RT kit, RevertAid, Thermo Scientific, Cat #K1691) quantitative PCR was performed with Taqman Master Mix (Thermo Scientific, Cat #4304437) and the following probes: Mm00457739 (Slc22a4), Mm00840361 (Slc47a1), Mm00525575 (Slc29a4), Mm00488294 (Slc22a3),

Mm00456303 (Slc22a1), Mm02601013 (Slc47a2), Mm00472657 (Slc19a3), Mm00457295 (Slc22a2), Mm00441468 (Slc22a5), Mm00439391 (Slc6a4), Mm00436661 (Slc6a2). MIQE guidelines were followed for the quantitative RT-PCR (Bustin et al., 2009).

Liquid Chromatography - Mass Spectrometry (LC-MS)

Metformin and metformin-d6 were purchased from Sigma Aldrich (Cat #PHR1084) and QMX laboratories (Cat #D-6012) and all solvents/additives were at least HPLC grade. Metformin was extracted as previously described (Jenkins *et al.*, 2020). Briefly, the samples were weighed/pipetted into plastic tubes (Eppendorf) with a 5 mm stainless steel ball. Then, 400 µL of chloroform: methanol (2:1, Sigma Aldrich, Cat #34854 and Cat #M/4056/17) solution was added. The samples were then homogenised using a Bioprep-24-1004 homogeniser (Allsheng) run at 4.5 m/s for 60 seconds. 100 µL of the metformin-d6 (1 µM in water) was added followed by the addition of 600 µL of chloroform: methanol (2:1) solution and 300 µL of water (Sigma Aldrich, Cat #1.15333). The samples were vortexed and centrifuged at ~21,000 g for 5 minutes. The aqueous extracts were transferred into glass vials and dried down using a Concentrator Plus (Eppendorf) run at 60^{o}C for 180 minutes. The samples were reconstituted in 100 µL of chromatography starting conditions and transferred into glass vial inserts for analysis. LC-MS analysis was achieved using a HPLC System (Shimadzu UK Limited) injecting 5 µL of the sample onto a Scherzo SM-C18 column (150 mm * 3 mm I.D., 3 µm) maintained at 40^{o}C. Mobile phase [A] was 30 mM ammonium acetate (Sigma Aldrich, Cat #17836) in water with 0.02% acetic acid (Sigma Aldrich, Cat # 222142500). Mobile phase [B] was 20% acetonitrile (Sigma Aldrich, Cat #34851**)**, 80% water with 0.8% acetic acid. The flow was maintained at 0.5 mL/min with the following gradient: 0.00 minutes_10% [B]; 0.20 min_10% [B]; 1.20 min_99% [B]; 5.00 min_99% [B]; 5.10 min_10% [B]; 8.00 min_10% [B]. The needle was washed using 50:50 water: acetonitrile solution. An Exactive Orbitrap with a heated electrospray ionisation source (Thermo Fisher Scientific) was calibrated before sample analysis. The instrument tune file (positive mode, full-scan: m/z 100 to 200, resolution: 2 Hz) was optimised for metformin and applied throughout the analysis.

Statistical analyses

The visual difference in body weight of control and obese dams means that it is not possible to blind the individual carrying out the physiological analysis to maternal group. However histological analysis was performed following coding and blinding of the sample group to the individual carrying out the analysis. One- and Two-Way ANOVA, Pearson correlation and paired t-test were performed with the GraphPad Prism 9.0.0 Software, statistical outliers were removed following Rout testing and n numbers are indicated below each Figure and mean ± SD presented in the text and the Figures. Assumptions for the use of parametric tests were tested via the Shapiro-Wilk test for normality and the Brown-Forsythe test for equal variance. The fasting insulin, ipGTT AUC, HOMA-IR and liver steatosis data showed unequal variance and therefore a Welch ANOVA was performed. All other data met the assumptions required. The heatmap, organisation of the data, calculations and linear models were performed in R Studio (Version 1.3.959). Random-effects models were constructed for the fetal data (using the lmer4 package in R) to account for litter structure as a random effect, with sex and the experimental group as fixed effects. Other possible co-variates, for example litter size and position within the uterus, did not significantly improve the fit of the model and were therefore not included in the final model for analysis. The model was used for the analysis of the fetal bodyweight, fetal biometrical measurements, the placental weight, the body weight to placental ratio where all fetuses in a litter were included for analysis, however for visualisation the mean ± SD is presented. For the analysis of the fetal liver weight, the placental structure (placental labyrinth and Calcium) and the umbilical artery pulsatility index one fetus per litter and sex was analysed and analysis performed with a Two-Way ANOVA with maternal environment and fetal sex as the independent variables. 14 control, 14 obese and 13 obese metformin-treated animals were included in this study (as this number provided sufficient power for all measurements other than ipGTT where 16 control, 20 obese and 19 obese metformin-treated animals were used), whenever a subset of these animals was used for a measure the n numbers are indicated in the figure legend or in the text if a figure is not shown.

Results

Equal concentrations of metformin are found in the maternal circulation and fetal circulation

Metformin concentrations in maternal serum (1.67 ± 2.05nmol/mL) on E18.5 of pregnancy were comparable to those previously reported in pregnant women being treated for GDM (Liao *et al.*, 2020). Furthermore similar concentrations were present in fetal plasma (2.06 ± 2.33 nmol/mL, n=13) and the placenta (109.7 ± 125.4 nmol/g, n=13) on E18.5 of pregnancy. There was therefore a strong positive correlation between maternal serum, fetal plasma, and placental metformin concentrations at this time point (Fig. 1*A, B*). Metformin was also detected at high levels in E13.5 placenta (143.8 ± 118.2 nmol/g, n=4). Consistent with the uptake of metformin into placental tissue, high levels of expression of 5 of the 11 known metformin transporters (Slc22a3, Slc22a4, Slc22a5, Slc6a2, and Slc6a4) were detected in the placenta at E18.5 (Fig. 1*C*). Of these Slc22a3 (Oct3), Slc6a2 (Net), Slc6a4 (Sert) were expressed at a higher level than Slc22a5 (Octn2) and Slc22a4 (Octn1) (Fig. 1*C*). Additional evidence for metformin passing into fetal circulation was demonstrated by its detection in fetal liver but also at significantly higher levels in fetal kidneys (Fig. 1*D*, p=0.02 via Mann-Whitney test). Accordingly, seven transporters were present in the fetal kidneys: Slc22a2 (Oct2), Slc22a3 (Oct3), Slc22a5 (Octn2), Slc6a4 (Sert), Slc47a1 (Mate1) and Slc22a1 (Oct1) (Fig 1*C*). In the liver only three transporters (Slc22a4 (Octn1), Slc47a1 (Mate1), Slc6a4 (Sert)) were detected (Fig. 1*C*). Consistent with highest observed levels of metformin and metformin transporters in the fetal kidneys, and consistent with urinary excretion, metformin was also detected at high concentrations in the amniotic fluid (Fig 1*D*).

Metformin treatment in obese dams reduces fat mass at the end of pregnancy

Dams randomised to the obesogenic diet were heavier throughout pregnancy compared to those randomised to control diet (Fig. 2*A*). At the end of gestation (E18.5), obese untreated dams had a significantly higher fat mass than the controls ($p<0.0001$, Fig. 2*B*). Supplementing the obese diet with metformin resulted in a significantly lower fat mass in the obese metformin-treated group compared to the obese untreated group at E18.5 ($p=0.02$, Fig. 2*B*).

Metformin supplementation to obese dams improves glucose tolerance and liver steatosis

Glucose levels after a 4-hour fast were not significantly different between the three groups (8.9 ± 1.4 mmol/l in control, 9.0 ± 1.9 mmol/l in obese and 10.0 ± 2.1 mmol/l in obese metformin-treated group, p=0.1 in One-Way ANOVA). However glucose tolerance at E17.5 (Fig. 2*C*) was impaired in the obese untreated dams compared to the controls (area under the curve (AUC): 526 ± 274 in obese untreated vs. 332 ± 108 in controls, p=0.02, n=16 and 20). Metformin treatment reduced the AUC of the obese dams (AUC: 380 ± 189 in obese metformin-treated n=19), so it was no longer different to the controls. Fasting insulin levels were increased in the obese untreated dams compared to controls (p=0.008, Fig. 2*D*), which was reduced with metformin treatment but still significantly increased compared to control dams (p=0.01, Fig. 2D). HOMA-IR was increased in the obese compared to controls (6.97 ±1.67 in control and 16.84 ±11.13 in obese dams, p=0.01) and remained increased compared to the controls after metformin treatment (14.78 ± 9.22 in metformin-treated dams, p=0.03 compared to controls). In addition to impaired glucose tolerance and insulin resistance, obese untreated dams displayed increased liver fat compared to control dams (p<0.0001). This was reduced by metformin treatment (p=0.01 versus obese untreated group) but remained increased compared to controls (p <0.001), Fig.2*E* and *F*). Overall, metformin treatment in pregnancy resulted in improved metabolic health of the obese pregnant females.

Metformin treatment in obese dams improves uterine artery compliance and reduces serum sFlt levels

Doppler ultrasound analysis of the uterine artery blood flow showed an increased pulsatility index (p=0.003) and increased resistance index (p=0.005) in the obese untreated dams compared to controls (Fig. 2*H, I*). The increased indices are indicative of high resistance in the vessel leading to impaired uterine artery blood flow. The increased uterine artery resistance in obese dams was rescued by metformin treatment. Both pulsatility and resistance index (p=0.04 and p=0.03 respectively) were significantly reduced in obese metformin-treated dams compared to obese untreated dams and no longer different to controls (p=0.5 and p=0.7 respectively, Fig. 2*H, I*). Maternal fasting insulin levels correlated positively with the uterine artery pulsatility

index (Fig. 2*J*). Serum sFlt levels (soluble VEGFR-1) were increased significantly in the obese untreated group compared to control dams (37.3 ± 12.2 ng/mL in obese untreated vs. 26.2 ± 10.5 ng/mL in controls, p=0.04, n=13 and 14). Metformin treatment of obese dams reduced sFlt levels (29.5 ± 10.7 ng/mL, n=12) to levels that were not significantly different to controls (p=0.7).

Fetuses from obese dams with and without metformin treatment are both symmetrically smaller than controls

Male and female fetuses from obese dams with and without metformin treatment weighed less compared to controls (P<0.001, Fig. 3*A*). Litter size was not significantly different between groups (7.9 ± 1.6 in control, 8.4 ± 1.7 in obese and 8.6 ± 1.2 in obese metformin-treated group, p=0.5 in One-Way ANOVA). The reduction in fetal weight was a result of symmetric growth restriction, with reductions of similar magnitudes in crown-rump-length, biparietal diameter, head length, abdominal transverse diameter and fetal liver weight (Fig. 3*B*-*G*). As expected, indices of growth were significantly lower in female fetuses compared to male fetuses (P <0.05). There were no significant differences in either the umbilical artery pulsatility index (Fig. 3*H*), the middle cerebral artery pulsatility index, or the cerebroplacental ratio (CPR) between any of the groups (data not shown). Placental pulsatility index (PPI), a measure for placental impedance and a tool to predict fetal growth restriction, was increased in the pregnancies of obese untreated and obese metformin-treated dams (Fig. 3*I*). The PPI was significantly correlated with fetal body weight (Fig. 3*J*).

Placentas from obese untreated and obese metformin-treated dams have reduced labyrinthine area and increased calcification

Male and female placentas from obese untreated but not obese metformin-treated dams were heavier compared to control placentas (p=0.007, Fig. 4*A*). The fetal bodyweight to placental weight ratio was reduced in both obese untreated and obese metformin-treated animals indicating reduced placental efficiency (p<0.001, Fig. 4*B*). Across all groups, placental efficiency was lower in male compared to female fetuses (p=0.001).
Male and female placentas from obese untreated dams had a reduced labyrinthine area (p<0.0001), the main nutrient exchange zone of the murine placenta (Fig. 4*C* and 4*D*).

This reduction was not prevented by metformin treatment (p=0.002, Fig. 4*D*). Reduced placental labyrinth is likely to be a contributor to the reduced fetal growth as shown by the correlation between the labyrinthine area of the placenta and fetal weight (Fig 4*E*). Placental calcification was observed solely in the obese untreated and obese metformin-treated groups but not in the control group (P<0.001 for control vs. obese untreated and obese metformin-treated group, Fig. 4*F*, *G*). In areas with calcium deposits, the labyrinthine structure was damaged (Fig. 4*H*).

Discussion

Exposure to a maternal high fat/high sugar diet resulted in a pronounced obesity phenotype and the subsequent development of glucose intolerance, insulin resistance, and reduced uterine artery compliance during pregnancy. Metformin treatment in our model resulted in improvement of maternal metabolic and vascular parameters but did not improve placental or fetal parameters.

Ultrasound imaging of the fetus and the uterine artery is commonly used to assess human pregnancies throughout gestation and a recent review highlighted the importance and new opportunities of pregnancy imaging in the field of developmental programming (Morrison *et al.*, 2021). The physiological drop in uterine artery PI via vascular remodelling during pregnancy is essential to enable low resistance placental blood flow and thus support fetal growth. In human pregnancy, maternal overweight/obesity is associated with an attenuation in the physiological drop in uterine artery PI (Teulings *et al.*, 2020) and there is increased likelihood of uterine artery PI above the normal range (Kim *et al.*, 2015). GDM has been associated with impairment of endothelium-dependent vasorelaxation (Knock *et al.*, 1997), which has been demonstrated in a murine GDM model with consequent increased uterine artery resistance (Stanley *et al.*, 2011). We show for the first time that our mouse model of maternal obesity recapitulates this, with increased levels of sFlt in the obese dams and reduced uterine artery compliance that correlates positively with maternal fasting insulin levels. Our obesity mouse model thereby recapitulates phenotypes of human obese pregnancies as obesity is a well-known risk factor for the development of preeclampsia (Roberts *et al.*, 2011). SFlt (VEGR-1), which is used as a biomarker for preeclampsia in humans, can bind vascular endothelial growth factor (VEGF) which leads to an angiogenic imbalance and endothelial dysfunction (Sones & Davisson, 2016). Metformin treatment in humans has previously been shown to reduce the incidence of preeclampsia and hypertensive disorders, potentially via increasing nitric oxide, improving endothelial dysfunction, and reducing sFlt secretion (Brownfoot *et al.*, 2016; Romero *et al.*, 2017; Soobryan *et al.*, 2018). In our model, metformin treatment improved uterine artery compliance and reduced sFlt in the maternal serum, adding novel evidence for metformin's potential to prevent preeclampsia and demonstrating that our model provides an important platform to further elucidate mechanisms. Future work in this

area will complement currently planned human trials of metformin for preeclampsia prevention (Cluver *et al.*, 2019).

Currently metformin is used to treat GDM in many settings, however there are wide global variations in clinical recommendations (Lindsay & Loeken, 2017). Long-term data about possible impacts of metformin use in pregnancy on offspring adiposity are starting to emerge, highlighting possible increased adiposity in mid-childhood following maternal metformin treatment (Tarry-Adkins *et al.*, 2019). Apart from teratology analyses that show no increased risk of fetal anomaly following maternal metformin exposure in pregnancy (Given *et al.*, 2018), little data exists from clinical studies regarding the direct impact of metformin on the placenta or fetus including growth (Tarry-Adkins *et al.*, 2019). The use of a mouse model allowed us to assess the effects of *in utero* exposure on the placenta and the fetus directly. Sheep and rodent models are commonly used in the field of developmental programming significantly reducing the time to generate valuable data regarding safe and efficient interventions during pregnancy (Dickinson *et al.*, 2016). The murine pregnancy is well-characterised and thereby differences between the human and the murine pregnancy are well-known. The fetal period compared to the embryonic period is much longer in humans compared with the mouse that is born less mature. This is apparent when looking at the fat tissue development at birth with 1-2% of fat in a mouse and 16% of fat in a newborn human (Widdowson, 1950). Although the human and the mouse both have chorioallantoic and hemochorial placentas, there are structural differences and the invasion of the placental trophoblast cells into the uterus is shallower in the mouse compared to the human (Schmidt *et al.*, 2015). However once the final placenta is established the labyrinthine zone in the mouse placenta and the chorionic villi in the human placenta are very similar with regards to the exchange mechanism between maternal and fetal blood (Rossant & Cross, 2001). The mouse is therefore a useful tool to address important questions in the field of developmental programming in relation to the placenta, such as those addressed in the current study.

In the current study, placentas from obese dams showed reduced placental efficiency, evidenced by increased calcium deposits, and reduced labyrinthine area. As the labyrinthine zone is the main exchange zone between the maternal and fetal circulation in the murine placenta the reduced size and the presence of calcium depositions is likely to reduce efficient nutrient transport to the fetus. Increased calcium depositions are

associated with placental ageing in human pregnancy and are often observed in placentas from obese and GDM-affected pregnancies highlighting that our model mimics features of human pregnancies (Salge *et al.*, 2012). Mechanistic insight into how reduced labyrinthine area might occur comes from recent transcriptomic analyses from our laboratory showing downregulation of transcripts involved in labyrinthine development in placentas from obese dams (De Barros Mucci *et al.*, 2020). We observed a strong correlation between reduced labyrinthine area, increased placental impedance (as measured by the PPI (Gudmundsson *et al.*, 2017)), and reduced fetal growth. Many different factors on the maternal (such as suboptimal nutrition or smoking) and fetal side (such as genetic factors) can be associated with fetal growth restriction but a common feature and driving factor is reduced uterine-placental perfusion and reduced fetal nutrition (Nardozza *et al.*, 2017). It is thereby striking that despite significant improvements in maternal metabolic health and uterine artery compliance with metformin treatment, the adverse impacts of maternal obesity on placental development were not rescued and fetal growth was still significantly restricted. We hypothesize that mechanisms driving the fetal growth restriction differ at least partially between the obese untreated and the obese metformin-treated pregnancies. Overall, the fetal weight and biometry data shows higher variation in the obese untreated and the obese metformin-treated group compared to the control group highlighting a different degree of response to the obesogenic diet and the metformin treatment. The maternal data highlights different degrees of obesity and glucose intolerance in our model that can be an explanation for the higher variability in these groups regarding fetal outcomes. In humans metformin treatment fails in 30-50% of women with GDM who then require additional insulin treatment (Tarry-Adkins *et al.*, 2020). A difference in the response to metformin treatment can therefore also explain increased variation in the metformin-treated group in our model.

We showed a strong correlation between metformin levels in the maternal and the fetal circulation and that circulating concentrations were equivalent. This result is consistent with human studies that demonstrate at least 50% of maternal metformin levels in fetal circulation (Priya & Kalra, 2018), with some studies showing equal or higher concentrations in the fetal circulation (Vanky *et al.*, 2005). Importantly, we demonstrate that as well as entering the fetal circulation, maternal administration of metformin also led to metformin uptake into fetal liver and kidney, both of which expressed high levels of known metformin transporters. Metformin was also present in the amniotic fluid,

highlighting that the fetus is repeatedly exposed to metformin by swallowing. The immediate and long-term consequences of direct fetal tissue exposure to metformin are unknown. Data on metformin treatment outside of pregnancy shows that metformin activates AMPK and can inhibit complex I in mitochondria at high concentrations. Activation of AMPK leads to reduced mTOR signalling, this is relevant in highly-mitotic tissues such as cancer where metformin can slow cell proliferation (Pernicova & Korbonits, 2014). Additionally, AMPK activation leads to reduced lipid synthesis and gluconeogenesis, mediating the beneficial effects on metabolic health in T2D patients (Rena *et al.*, 2017). Recent data shows that metformin increases GDF-15 which increases energy expenditure and reduces food intake and thereby body weight (Coll *et al.*, 2020). It is possible that metformin has similar actions on fetal and placental tissues leading to altered metabolism and growth, especially given the high degree of cell proliferation and division during development (Nguyen *et al.*, 2018). This could contribute to the observed reduction in fetal growth despite the correction of uterine blood flow by metformin. It has been hypothesized that metformin may also have epigenetic effects on the fetus that could have long term health consequences via changes in activity of histone modification enzymes or DNA methylation (Claire *et al.*, 2018; Owen *et al.*, 2021). This highlights the complexity of metformin use *in utero* and the need for further research.

In conclusion, our study demonstrates that metformin has beneficial effects on maternal metabolic health and, consistent with human data, has the potential to prevent preeclampsia. However, despite the beneficial effects on maternal physiology, it did not prevent obesity-induced placental ageing and fetal growth restriction. Moreover, metformin enters the fetal circulation and highly proliferative fetal tissues, the long term implications of which are currently unknown. These findings highlight the complex balance of risk versus benefits that are weighed in obstetric medical treatments and provide a well-characterised platform for further mechanistic research on pregnancies complicated by obesity and/or GDM and on the actions of metformin in pregnancy.

Additional information

Data Availability

All analysed data can be found in the manuscript, raw datasets are available upon request.

Competing interests

The authors declare that they have no competing interests.

Author Contributions

AH, DSF and SEO designed research; AH, DSF, HLB, TA performed research; BJ and AK performed LC-MS analysis; RAH and IPH provided intellectual input; AH analysed data and wrote the paper with input from DSF, CEA and SEO. All authors read, commented on, and approved the final version of the manuscript.

Acknowledgements

We would like to thank C. Custance (University of Cambridge Metabolic Research Laboratories and MRC Metabolic Diseases Unit, Wellcome Trust-MRC Institute of Metabolic Science, Addenbrooke's Hospital, Cambridge, UK) for expert technical assistance. We would like to thank the histology core (J. Warner, MRC Metabolic Diseases Unit) and B. Mahler-Araujo (Histopathology Addenbrookes) for their expert histology advice. We would also like to acknowledge the imaging core of the Institute of Metabolic Science (G. Strachan) and the Metabolomics and Lipidomics Laboratory core (NIHR Cambridge Biomedical Research Centre).

We also thank Dr. N. Shreeve and Dr. C. Murdoch for their help in setting up murine uterine and fetal ultrasound.

Funding

This work was supported by the BHF [PG/13/46/30329] and the MRC [MC_UU_00014/4]. CEA is supported by a Medical Research Council New Investigator Grant (MR/T016701/1). AH was supported by a Wellcome Trust studentship [108926/B/15/Z]. SEO is a member of the Cambridge BHF Centre of Research Excellence [RE/18/1/34212]. SEO and DSFT are supported by the Medical Research Council (MC_UU_12012/4) and the British Heart Foundation (RG/17/12/33167).

The histology core is funded by the MRC [MC_UU_00014/5] and imaging core of the Institute of Metabolic Science by a Wellcome Major Award [208363/Z/17/Z].

This research was funded in part by the Wellcome Trust [108926/B/15/Z]. For the purpose of open access, the author has applied a CC BY public copyright licence to any Author Accepted Manuscript version arising from this submission.

660 **Literature**

661 Alfaradhi MZ, Fernandez-Twinn DS, Martin-Gronert MS, Musial B, Fowden A &
662 Ozanne SE (2014). Oxidative stress and altered lipid homeostasis in the
663 programming of offspring fatty liver by maternal obesity. *Am J Physiol - Regul*
664 *Integr Comp Physiol* **307,** R26–R34.

665 Alfaradhi MZ & Ozanne SE (2011). Developmental programming in response to
666 maternal overnutrition. *Front Genet*; DOI: 10.3389/fgene.2011.00027.

667 American Diabetes Association (2019). 14. Management of diabetes in pregnancy:
668 Standards of Medical Care in Diabetes-2019. *Diabetes Care* **42,** S165–S172.

669 De Barros Mucci D, Kusinski LC, Wilsmore P, Loche E, Pantaleão LC, Ashmore TJ,
670 Blackmore HL, Fernandez-Twinn DS, Das Graças T. do Como M & Ozanne SE
671 (2020). Impact of maternal obesity on placental transcriptome and morphology
672 associated with fetal growth restriction in mice. *Int J Obes* **44,** 1087–1096.

673 Blackmore HL, Niu Y, Fernandez-Twinn DS, Tarry-Adkins JL, Giussani DA & Ozanne
674 SE (2014). Maternal diet-induced obesity programs cardiovascular dysfunction in
675 adult male mouse offspring independent of current body weight. *Endocrinology*
676 **155,** 3970–3980.

677 Brownfoot FC, Hastie R, Sc Bb, Hannan NJ, Sci B, Cannon P, Tuohey L, Parry LJ,
678 Senadheera S, Illanes SE, Kaitu uhevaha J & Tong S (2016). Metformin as a
679 prevention and treatment for preeclampsia: effects on soluble fms-like tyrosine
680 kinase 1 and soluble endoglin secretion and endothelial dysfunction. *Am J Obstet*
681 *Gynecol* **214,** e1–e15.

682 Bustin SA, Benes V, Garson JA, Hellemans J, Huggett J, Kubista M, Mueller R, Nolan
683 T, Pfaffl MW, Shipley GL, Vandesompele J & Wittwer CT (2009). The MIQE
684 guidelines: Minimum information for publication of quantitative real-time PCR
685 experiments. *Clin Chem* **55,** 611–622.

686 Claire S, Mbiomed B, Gaewyn |, Ellison Pgraddipbiomed C, Melton PE, Newsholme P,
687 Desire C & Mamotte S (2018). Epigenetic effects of metformin: From molecular
688 mechanisms to clinical implications. ; DOI: 10.1111/dom.13262.

689 Cluver C, Walker SP, Mol BW, Hall D, Hiscock R, Brownfoot FC, Kaitu'U-Lino TJ &
690 Tong S (2019). A double blind, randomised, placebo-controlled trial to evaluate

the efficacy of metformin to treat preterm pre-eclampsia (PI2 Trial): Study protocol. *BMJ Open* **9,** e025809.

Coll AP et al. (2020). GDF15 mediates the effects of metformin on body weight and energy balance. *Nature* **578,** 444–448.

David McIntyre H, Catalano P, Zhang C, Desoye G, Mathiesen ER & Damm P (2019). Gestational diabetes mellitus. *Nat Rev Prim*; DOI: 10.1038/s41572-019-0098-8.

Deeney S, Powers KN & Crombleholme TM (2016). A comparison of sexing methods in fetal mice. *Lab Anim* **45,** 380–384.

Desoye G & Wells JCK (2021). Pregnancies in Diabetes and Obesity: The Capacity-Load Model of Placental Adaptation. *Diabetes* **70,** 823–830.

Dickinson H, Moss TJ, Gatford KL, Moritz KM, Akison L, Fullston T, Hryciw DH, Maloney CA, Morris MJ, Wooldridge AL, Schjenken JE, Robertson SA, Waddell BJ, Mark PJ, Wyrwoll CS, Ellery SJ, Thornburg KL, Muhlhausler BS & Morrison JL (2016). A review of fundamental principles for animal models of DOHaD research: An Australian perspective. *J Dev Orig Health Dis* **7,** 449–472.

Feig DS et al. (2020). Articles Metformin in women with type 2 diabetes in pregnancy (MiTy): a multicentre, international, randomised, placebo-controlled trial. *Lancet Diabetes Endocrinol* **8,** 834–844.

Fernandez-Twinn DS, Blackmore HL, Siggens L, Giussani DA, Cross CM, Foo R & Ozanne SE (2012). The programming of cardiac hypertrophy in the offspring by maternal obesity is associated with hyperinsulinemia, AKT, ERK, and mTOR activation. *Endocrinology* **153,** 5961–5971.

Gaillard R (2015). Maternal obesity during pregnancy and cardiovascular development and disease in the offspring. *Eur J Epidemiol* **30,** 1141–1152.

Given JE, Loane M, Garne E, Addor M-C, Bakker M, Bertaut-Nativel B, Gatt M, Klungsoyr K, Lelong N, Morgan M, Neville AJ, Pierini A, Rissmann A & Dolk H (2018). Metformin exposure in first trimester of pregnancy and risk of all or specific congenital anomalies: exploratory case-control study. *BMJ* **361,** 2477.

Gray SG, McGuire TM, Cohen N & Little PJ (2017). The emerging role of metformin in gestational diabetes mellitus. *Diabetes Obes Metab* **19,** 765–772.

721 Grundy D (2015). Principles and standards for reporting animal experiments in The
722 Journal of Physiology and Experimental Physiology. *J Physiol* **593,** 2547–2549.
723 Available at: http://www.physoc.org/animal-experiments [Accessed July 4, 2021].

724 Gudmundsson S, Flo K, Ghosh G, Wilsgaard T & Acharya G (2017). Placental
725 pulsatility index: a new, more sensitive parameter for predicting adverse outcome
726 in pregnancies suspected of fetal growth restriction. *Acta Obstet Gynecol Scand* **96,**
727 216–222.

728 Guro L, Hanem E, Stridsklev S, Júlíusson PB, Salvesen Ø, Roelants M, Carlsen SM,
729 Ødegård R, Vanky E, Hanem LG & Phd ØS (2018). Metformin use in PCOS
730 pregnancies increases the risk of offspring overweight at 4 years of age; follow-up
731 of two RCTs. *J Clin Endocrinol Metab* **103,** 1612–1621.

732 Hayes EK, Lechowicz A, Petrik JJ, Storozhuk Y, Paez-Parent S, Dai Q, Samjoo IA,
733 Mansell M, Gruslin A, Holloway AC & Raha S (2012). Adverse fetal and neonatal
734 outcomes associated with a life-long high fat diet: Role of altered development of
735 the placental vasculature. *PLoS One* **7,** e33370.

736 Hernandez-Andrade E, Ahn H, Szalai G, Korzeniewski SJ, Wang B, King M,
737 Chaiworapongsa T, Than NG & Romero R (2014). Evaluation of utero-placental
738 and fetal hemodynamic parameters throughout gestation in pregnant mice using
739 high-frequency ultrasound. *Ultrasound Med Biol* **40,** 351–360.

740 Hill B, Skouteris H, Teede HJ, Bailey C, Baxter J-AB, Bergmeier HJ, Borges ALV,
741 Harrison CL, Jack B, Jorgensen L, Lim S, Montanaro C, Redman L, Steegers E,
742 Stephenson J, Sundseth H, Thangaratinam S, Walker R & Boyle JA (2019). Health
743 in Preconception, Pregnancy and Postpartum Global Alliance: International
744 Network Preconception Research Priorities for the Prevention of Maternal Obesity
745 and Related Pregnancy and Long-Term Complications. *J Clin Med* **8,** 2119.

746 Holmgren M, Wåhlin A, Dunås T, Malm J & Eklund A (2020). Assessment of Cerebral
747 Blood Flow Pulsatility and Cerebral Arterial Compliance With 4D Flow MRI. *J*
748 *Magn Reson Imaging* **51,** 1516–1525.

749 Hu Z, Tylavsky FA, Han JC, Kocak M, Fowke JH, Davis RL, Lewinn K, Bush NR &
750 Zhao Q (2019). Maternal metabolic factors during pregnancy predict early
751 childhood growth trajectories and obesity risk: the CANDLE Study. *Int J Obes* **43,**

1914–1922.

Isganaitis E, Woo M, Ma H, Chen M, Kong W, Lytras A, Sales V, DeCoste-Lopez J, Lee KJ, Leatherwood C, Lee D, Fitzpatrick C, Gall W, Watkins S & Patti ME (2014). Developmental programming by maternal insulin resistance: Hyperinsulinemia, glucose intolerance, and dysregulated lipid metabolism in male offspring of insulin-resistant mice. *Diabetes* **63,** 688–700.

Janssen BJA, De Celle T, Debets JJM, Brouns AE, Callahan MF & Smith TL (2004). Effects of anesthetics on systemic hemodynamics in mice. *Am J Physiol - Hear Circ Physiol* **287,** 1618–1624.

Jarvie E, Hauguel-de-Mouzon S, Nelson SM, Sattar N, Catalano PM & Freeman DJ (2010). Lipotoxicity in obese pregnancy and its potential role in adverse pregnancy outcome and obesity in the offspring. *Clin Sci (Lond)* **119,** 123–129.

Jenkins B, Ronis M & Koulman A (2020). Lc–ms lipidomics: Exploiting a simple high-throughput method for the comprehensive extraction of lipids in a ruminant fat dose-response study. *Metabolites* **10,** 1–27.

Kim YH, Lee HJ, Shin JE, Lee Y, Shin JC, Park TC & Park IY (2015). The predictive value of the uterine artery pulsatility index during the early third trimester for the occurrence of adverse pregnancy outcomes depending on the maternal obesity. *Obes Res Clin Pract* **9,** 374–381.

Knock GA, McCarthy AL, Lowy C & Poston L (1997). Association of gestational diabetes with abnormal maternal vascular endothelial function. *BJOG An Int J Obstet Gynaecol* **104,** 229–234.

Lahti-Pulkkinen M, Bhattacharya S, Wild SH, Lindsay RS, Räikkönen K, Norman JE, Bhattacharya S & Reynolds RM (2019). Consequences of being overweight or obese during pregnancy on diabetes in the offspring: a record linkage study in Aberdeen, Scotland. *Diabetologia* **62,** 1412–1419.

Liao MZ, Flood Nichols SK, Ahmed M, Clark S, Hankins GD, Caritis S, Venkataramanan R, Haas D, Quinney SK, Haneline LS, Tita AT, Manuck T, Wang J, Thummel KE, Brown LM, Ren Z, Easterling TR & Hebert MF (2020). Effects of Pregnancy on the Pharmacokinetics of Metformin. *Drug Metab Dispos* **48,** 264–271.

Lindsay RS & Loeken MR (2017). Metformin use in pregnancy: promises and uncertainties. *Diabetologia* **60,** 1612–1619.

Maragkoudaki X, Naylor M, Papacleovoulou G, Stolarczyk E, Rees D, Pombo JM, Abu-Hayyeh S, Czajka A, Howard JK, Malik AN, Williamson C, Poston L & Taylor PD (2020). Supplementation with a prebiotic (polydextrose) in obese mouse pregnancy improves maternal glucose homeostasis and protects against offspring obesity. *Int J Obes* **44,** 2382–2393.

Mcfarlane L, Truong V, Palmer JS, Wilhelm D, Schmid M & Wilhelm D (2013). E-Mail Novel PCR Assay for Determining the Genetic Sex of Mice. *Sex Dev* **7,** 380–384.

Mitanchez D, Yzydorczyk C, Siddeek B, Boubred F, Benahmed M & Simeoni U (2015). The offspring of the diabetic mother e Short-and long-term implications. *Best Pract Res Clin Obstet Gynaecol* **29,** 256–269.

Morrison JL, Ayonrinde OT, Care AS, Clarke GD, Darby JRT, David AL, Dean JM, Hooper SB, Kitchen MJ, MacGowan CK, Melbourne A, McGillick E V., McKenzie CA, Michael N, Mohammed N, Sadananthan SA, Schrauben E, Regnault TRH & Velan SS (2021). Seeing the fetus from a DOHaD perspective: Discussion paper from the advanced imaging techniques of DOHaD applications workshop held at the 2019 DOHaD World Congress. *J Dev Orig Health Dis* **12,** 153–167.

Nardozza LMM, Caetano ACR, Zamarian ACP, Mazzola JB, Silva CP, Marçal VMG, Lobo TF, Peixoto AB & Araujo Júnior E (2017). Fetal growth restriction: current knowledge. *Arch Gynecol Obstet* **295,** 1061–1077.

Nguyen L, Chan S-Y, Kee A & Teo K (2018). Metformin from mother to unborn child - Are there unwarranted effects? ; DOI: 10.1016/j.ebiom.2018.08.047.

NICE (The National Institute for Health and Care Excellence) (2015). *Diabetes in pregnancy: management from preconception to the postnatal period*. Available at: https://www.nice.org.uk/guidance/ng3 [Accessed April 30, 2020].

Ochi H, Kusanagi Y, Katayama T, Matsubara K & Ito M (2003). Clinical significance of normalization of uterine artery pulsatility index with maternal heart rate for the evaluation of uterine circulation in pregnancy-induced hypertension. *Ultrasound*

Obstet Gynecol **21,** 459–463.

Orchard GE (2013). Pigments and minerals. In *Bancroft's Theory and Practice of Histological Techniques*, pp. 239–270. Elsevier.

Owen MD, Baker BC, Scott EM & Forbes K (2021). Interaction between Metformin , Folate and Vitamin B 12 and the Potential Impact on Fetal Growth and Long-Term Metabolic Health in Diabetic Pregnancies. 1–27.

Pantham P, Aye ILMH & Powell TL (2015). Inflammation in maternal obesity and gestational diabetes mellitus. *Placenta* **36,** 709–715.

Pernicova I & Korbonits M (2014). Metformin-mode of action and clinical implications for diabetes and cancer. *Nat Publ Gr* **10,** 143–156.

Priya G & Kalra S (2018). Metformin in the management of diabetes during pregnancy and lactation. *Drugs Context* **7,** 212523.

Rena G, Hardie DG & Pearson ER (2017). The mechanisms of action of metformin. *Diabetologia* **60,** 1577–1585.

Roberts JM, Bodnar LM, Patrick TE & Powers RW (2011). The Role of Obesity in Preeclampsia. *Pregnancy Hypertens* **1,** 6–16.

Romero R, Hüttemann M, Maymon E, Panaitescu B, Conde-Agudelo A, Pacora P, Yoon BH & Grossman LI (2017). Metformin, the aspirin of the 21 st century: its role in gestational diabetes, prevention of preeclampsia and cancer, and the promotion of longevity HHS Public Access. *Am J Obs Gynecol* **217,** 282–302.

Rossant J & Cross JC (2001). Placental development: Lessons from mouse mutants. *Nat Rev Genet* **2,** 538–548.

Rowan JA, Rush EC, Obolonkin V, Battin M, Wouldes T & Hague WM (2011). Metformin in gestational diabetes: the offspring follow-up (MiG TOFU): body composition at 2 years of age. *Diabetes Care* **34,** 2279–2284.

Salge AKM, Rocha KMN, Xavier RM, Ramalho WS, Rocha ÉL, Guimarães JV, Silva RCR e, Siqueira KM, Abdalla DR, Michelin MA & Murta EFC (2012). Macroscopic placental changes associated with fetal and maternal events in diabetes mellitus. *Clinics (Sao Paulo)* **67,** 1203–1208.

Salomäki H, Vä Hä Talo LH, Laurila K, Jä Ppinen NT, Penttinen A-M, Ailanen L, Ilyasizadeh J, Pesonen U, Koulu M & Aguila MB (2013). Prenatal Metformin Exposure in Mice Programs the Metabolic Phenotype of the Offspring during a High Fat Diet at Adulthood. *PLoS One* **8,** e56594.

Samuelsson AM, Matthews PA, Argenton M, Christie MR, McConnell JM, Jansen EHJM, Piersma AH, Ozanne SE, Twinn DF, Remacle C, Rowlerson A, Poston L & Taylor PD (2008). Diet-induced obesity in female mice leads to offspring hyperphagia, adiposity, hypertension, and insulin resistance: A novel murine model of developmental programming. *Hypertension* **51,** 383–392.

Schäfer-Graf UM, Gembruch U, Kainer F, Groten T, Hummel S, Hösli I, Grieshop M, Kaltheuner M, Bührer C, Kautzky-Willer A, Laubner K & Bancher-Todesca D (2018). Gestational Diabetes Mellitus (GDM), Diagnosis, Treatment and Follow-Up. Guideline of the DDG and DGGG (S3 Level, AWMF Registry Number 057/088, February 2018). *Geburtshilfe Frauenheilkd* **78,** 1219–1231.

Schmidt A, Morales-Prieto DM, Pastuschek J, Fröhlich K & Markert UR (2015). Only humans have human placentas: molecular differences between mice and humans. *J Reprod Immunol* **108,** 65–71.

SEMT (The Society of Endocrinology and Metabolism of Turkey) (2019). Clinical Practice Guideline for Diagnosis, Treatment and Follow-up of Diabetes Mellitus and Its Complications, 2019. 1–268. Available at: https://temd.org.tr/admin/uploads/tbl_kilavuz/20191107144832-2019tbl_kilavuz7c65cb4e70.pdf [Accessed March 3, 2021].

SMFM (The Society for Maternal-Fetal Medicine) (2018). SMFM Statement: Pharmacological treatment of gestational diabetes. *Am J Obstet Gynecol* **218,** B2–B4.

Sones JL & Davisson RL (2016). Preeclampsia, of mice and women. *Physiol Genomics* **48,** 565–572.

Soobryan N, Murugesan S, Pandiyan A, Moodley J & Mackraj I (2018). Angiogenic Dysregulation in Pregnancy-Related Hypertension—A Role for Metformin. *Reprod Sci* **25,** 1531–1539.

Stanley JL, Cheung CC, Sankaralingam S, Baker PN & Davidge ST (2011). Effect of

874 Gestational Diabetes on Maternal Artery Function. *Reprod Sci* **18,** 342–352.

875 Steculorum SM & Bouret SG (2011). Maternal diabetes compromises the organization
876 of hypothalamic feeding circuits and impairs leptin sensitivity in offspring.
877 *Endocrinology* **152,** 4171–4179.

878 Stephenson J, Heslehurst N, Hall J, J M Schoenaker DA, Hutchinson J, Cade JE, Poston
879 L, Barrett G, Crozier SR, Barker M, Kumaran K, Yajnik CS, Baird J & Mishra GD
880 (2018). Preconception health 1 Before the beginning: nutrition and lifestyle in the
881 preconception period and its importance for future health. *Lancet* **391,** 1830–1841.

882 Syngelaki A, Nicolaides KH, Balani J, Hyer S, Akolekar R, Kotecha R, Pastides A &
883 Shehata H (2016). Metformin versus Placebo in Obese Pregnant Women without
884 Diabetes Mellitus. *N Engl J Med* **374,** 434–443.

885 Tarry-Adkins JL, Aiken CE & Ozanne SE (2019). Neonatal, infant, and childhood
886 growth following metformin versus insulin treatment for gestational diabetes: A
887 systematic review and meta-analysis. *PLoS Med* **16,** e1002848.

888 Tarry-Adkins JL, Aiken CE & Ozanne SE (2020). Comparative impact of
889 pharmacological treatments for gestational diabetes on neonatal anthropometry
890 independent of maternal glycaemic control: A systematic review and meta-
891 analysis. *PLoS Med*; DOI: 10.1371/journal.pmed.1003126.

892 Teulings NEWD, Wood AM, Sovio U, Ozanne SE, Smith GCS & Aiken CE (2020).
893 Independent influences of maternal obesity and fetal sex on maternal
894 cardiovascular adaptation to pregnancy: a prospective cohort study. *Int J Obes* **44,**
895 2246–2255.

896 Vanky E, Zahlsen K, Spigset O & Carlsen SM (2005). Placental passage of metformin
897 in women with polycystic ovary syndrome. *Fertil Steril* **83,** 1575–1578.

898 Widdowson BEM (1950). Chemical composition of newly born mammals. *Nature* **166,**
899 626–628.

900 Zhang J & Croy A (2009). Using Ultrasonography to Define Fetal-Maternal
901 Relationships: Moving from Humans to Mice. *Comp Med* **59,** 527–553.

902

903

Figures

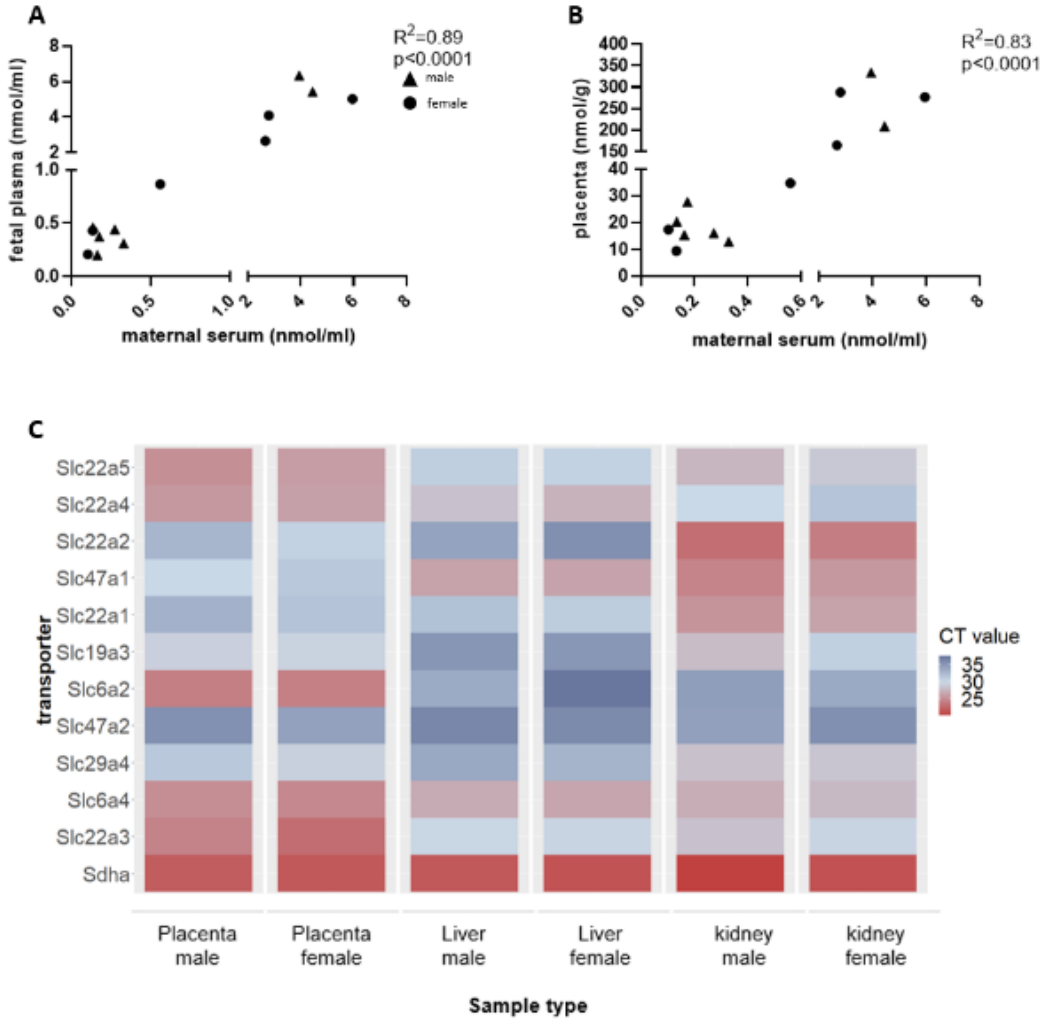

D

Sample type (E18.5)	metformin (mean ± SD)
fetal kidney	189.3 ± 207.7 nmol/g
fetal liver	17.9 ± 21.57 nmol/g
placenta	109.7 ± 125.4 nmol/g
amniotic fluid	21.89 ± 28.22 nmol/ml
Maternal serum	1.67 ± 2.05 nmol/ml
Fetal plasma	2.06 ± 2.33 nmol/ml

Figure 1: Metformin given to the obese mum during pregnancy can reach the fetal circulation and fetal tissues (A) Metformin concentrations measured in maternal serum were correlated with fetal plasma concentrations and (B) metformin levels in the placenta, circles represent female, triangles represent male fetuses. Linear regression and Pearson correlation coefficient R^2 are shown. (C) Expression of ten transporters

(known for their ability to transport metformin) was analysed in E18.5 placenta, fetal liver and fetal kidney, n=3 per tissue type and sex respectively. Raw CT values are shown, ranging from high expression (low Ct values, red color) to low expression (high CT values, blue color). (D) Metformin was measured in fetal kidney, liver, amniotic fluid (n=3 female and n=3 male) and placentas (n=7 male, n=6 female) via LC-MS, fluid samples are expressed in nmol/mL and tissue samples in nmol/mg to allow an approximate comparison.

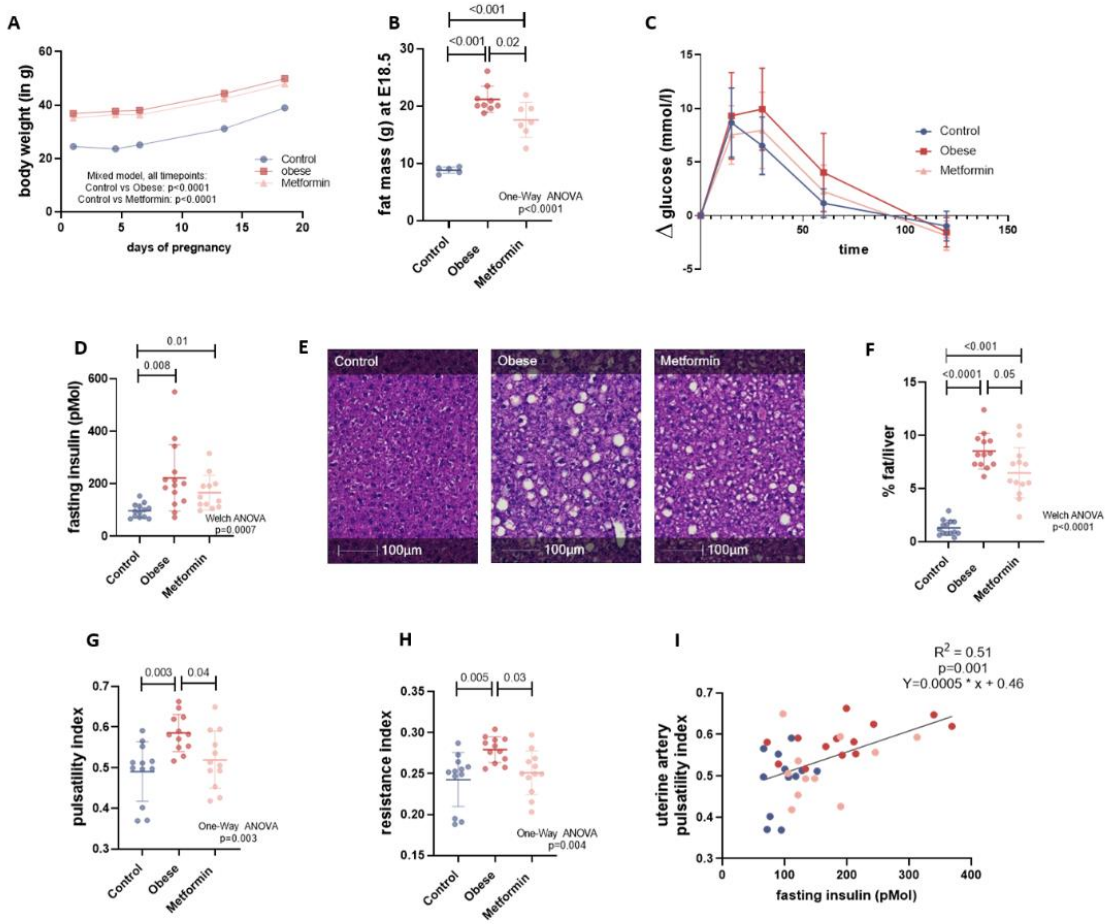

Figure 2: Maternal characteristics (A) Bodyweight of the dams was measured at day of the plug (E0.5), day 4.5, 6.5, 13.5 and 18.5 of gestation (n=14 for control, n=14 for obese, n=13 for metformin dams), mean ± SD and mixed model analysis is shown. (B) On day 18.5 fat mass was measured via TD-NMR (n=5 for control, n=9 for obese, n=7 for metformin dams). (C). An ipGTT was performed after a 4-hour fast on day 17.5 of pregnancy and glucose levels were measured and presented as the difference to the starting glucose level (n=16 for control, n=20 for obese, n=19 for metformin dams). (D) Fasting insulin levels were measured and mean ± SD and Welch ANOVA analysis are

shown (n=13 for control, n=14 for obese, n=13 for metformin dams). (E) Liver sections were stained with Haematoxylin and Eosin (representative images shown) and (F) the fat vacuole content quantified with HALO image analysis platform as a percentage of the whole liver section (n=14 for control, n=13 for obese, n=14 for metformin dams). (G) Pulsatility and (H) resistance indices were calculated and corrected for individual maternal heart rates (n=12 for all three groups). (I) Fasting insulin levels were correlated with uterine artery pulsatility index and linear correlation and Pearson correlation coefficient R^2 are shown. If not indicated differently statistical analyses in the figure show One-Way ANOVA followed by Tukey's multiple comparison test, error bars show mean ± SD.

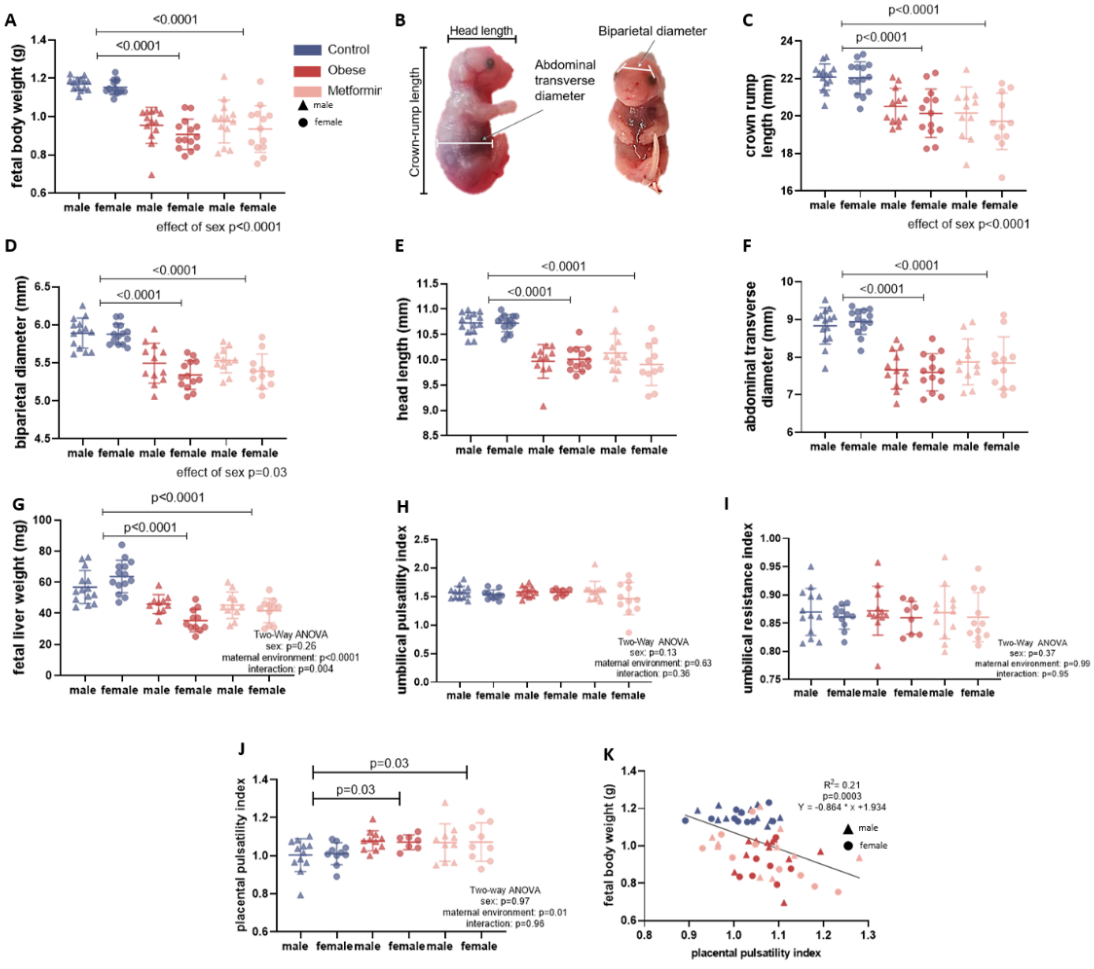

Figure 3: Fetuses from obese untreated and obese metformin-treated dams show symmetric growth restriction (A) Fetal weight was taken at E18.5 (male/female control fetuses from n=14/14 dams, male/female obese from n=13/14 dams and male/female metformin fetuses from n=13/13 dams). (B) Fetal biometry was performed

as shown and (C) crown-rump length, (D) biparietal diameter, (E) head length and (F) abdominal transverse diameter measured. For the fetal biometry n=14 dams for male and female control, n=12/13 dams for male/female obese and n=11 dams for male and female metformin fetuses are shown. Analysis is performed with a linear mixed model accounting for the dam as a random effect, in the graphs the mean ± SD per litter and sex is shown. (G) Fetal liver weights were taken at E18.5 in female and male control fetuses from n=14 dams, female/male obese fetuses from n=10/11 dams and female and male metformin fetuses from n=11 dams, mean ± SD and Two-Way ANOVA analysis is shown. (H) The umbilical pulsatility index (PI) and (I) resistance index were measured via ultrasound, analysis shows n=13 dams for male and n=11 dams for female control, n=12 dams for male and n= 8 dams for female obese and n=12 dams for male and n=11 dams for female metformin fetuses and Two-Way ANOVA (sex and maternal environment) with Tukey's multiple comparison test. (J) The placental pulsatility index (PPI) was calculated via the following formula: mean uterine artery PI + mean umbilical artery PI) / 2, n=12 dams for male and n=10 dams for female control, n=11 dams for male and n=7 dams for female obese and n=10 dams for male and n=9 for female metformin fetuses, Two-Way ANOVA analysis is shown. (K) The PPI was correlated with the fetal body weight, linear correlation and Pearson correlation coefficient R^2 are shown.

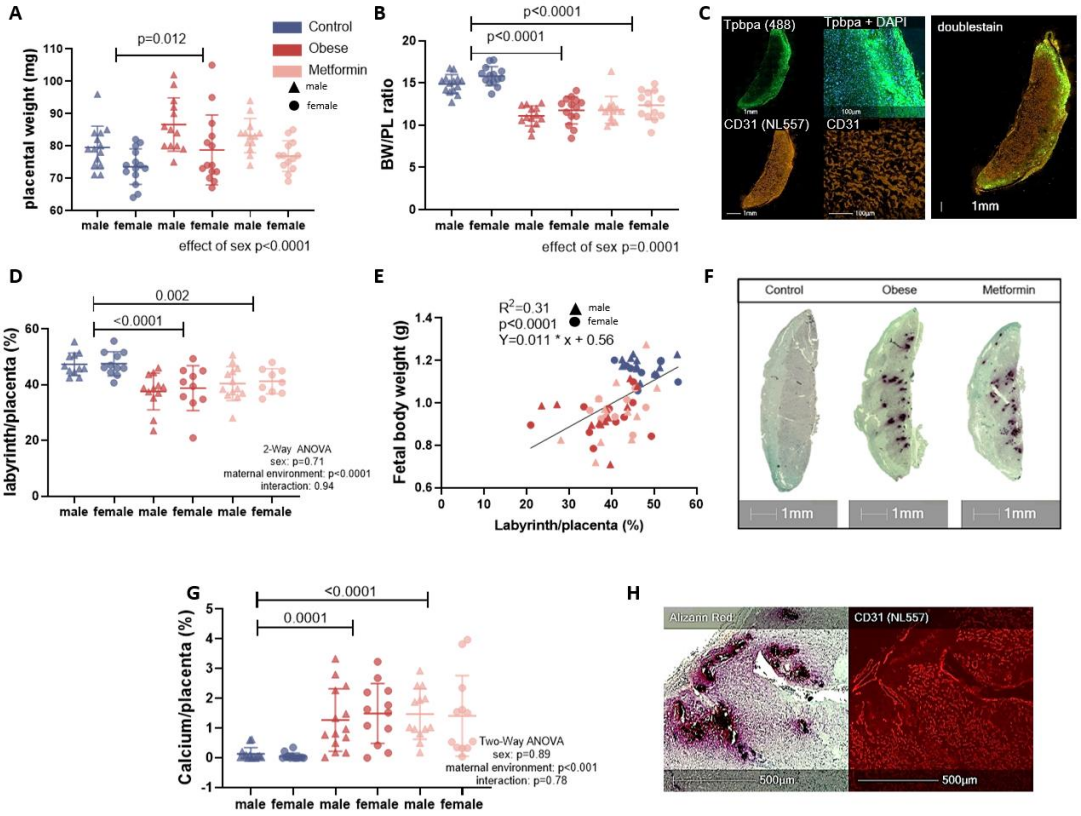

963

964 **Figure 4: Placentas from obese untreated and obese metformin-treated animals**
965 **show pathologies that can explain reduced efficiency** (A) Placentas were weighed on
966 the day of dissection (E18.5) and as an indicator of placental efficiency (B) the ratio of
967 body to placental weight was calculated (n=14 dams for male and female control,
968 n=13/14 dams for male/female obese and n=13 dams for male and female metformin
969 placentas). (C) Placental sections were stained for the trophoblast cell marker Tpbpa
970 and the endothelial cell marker CD31 via immunohistochemistry to allow delineation of
971 the trophoblast and labyrinthine layer of the placenta (n=11 dams for male and female
972 control, n=12/10 dams for male/female obese and n=13/9 dams for male/female
973 metformin placentas). (D) The percentage of labyrinth to the whole placenta was then
974 calculated. (E) Fetal body weight was correlated with the labyrinthine area of the
975 placenta from that individual fetus, one male and one female fetus per litter was
976 analysed, linear correlation and Pearson correlation coefficient R^2 are shown. (F) The
977 placentas were additionally stained for calcification with an Alizarin Red stain. (G) The
978 areas stained with Alizarin Red are quantified and expressed as a percentage of the
979 whole placenta (n=14 dams for male and female control, n=13/14 dams for male/female
980 obese and n=13/12 dams for male/female metformin placentas). (H) In areas with
981 calcium deposition the labyrinthine structure was damaged. Mean ± SD is shown and

Two-Way ANOVA (sex and maternal environment) is performed with a Tukey's multiple comparison test.